Gulf Stream Moisture Fluxes Impact Atmospheric Blocks Throughout the Northern Hemisphere

J. P. Mathews[1], A. Czaja[1], F. Vitart[2], and C. Roberts[2]

[1]Imperial College London
[2]European Centre for Medium-Range Weather Forecasts

Key Points:

- Gulf Stream moisture flux suppression reduces atmospheric blocking across the northern hemisphere.
- Gulf Stream moisture fluxes generate larger jet stream perturbations, fostering faster westward-propagating Rossby waves.
- Higher resolution models enhance signal transport from the boundary layer to the upper troposphere.

Corresponding author: Jamie Mathews, jamie.mathews19@imperial.ac.uk

Abstract

In this study, we explore the impact of oceanic moisture fluxes on atmospheric blocks using the ECMWF Integrated Forecast System. Artificially suppressing surface latent heat flux over the Gulf Stream region leads to a significant reduction (up to 30%) in atmospheric blocking frequency across the northern hemisphere. Affected blocks show a shorter lifespan (-6%), smaller spatial extent (-12%), and reduced intensity (-0.4%), with an increased detection rate (+17%). These findings are robust across various blocking detection thresholds. Analysis indicates a resolution-dependent response, with resolutions lower than Tco639 (∼18km) showing no significant change in some blocking characteristics, even with reduced blocking frequency. Exploring the broader Rossby wave pattern, we observe that diminished moisture flux favours eastward propagation and higher zonal wavenumbers, while air-sea interactions promotes stationary and westward-propagating waves with zonal wavenumber 3. This study underscores the critical role of western boundary current's moisture fluxes in modulating atmospheric blocking.

1 Forecast Dates

Table 1. Initial dates used for the reforecasts and the date the first block was detected over the North Atlantic in ERA5 data. Winter reforecasts are depicted in **bold**.

Initial Dates	Block Detected
10^{th} December 2009	13^{th} December 2009
9^{th} December 2010	13^{th} December 2010
27^{th} December 2016	30^{th} December 2016
14^{th} May 2018	17^{th} May 2018
30^{th} March 2019	2^{nd} April 2019
19^{th} May 2019	22^{nd} May 2019
20^{th} June 2019	23^{rd} June 2019
20^{th} July 2019	24^{th} July 2019
11^{th} September 2019	14^{th} September 2019
14^{th} October 2019	18^{th} October 2019
19^{th} November 2019	22^{nd} November 2019
27^{th} November 2019	30^{th} November 2019
12^{th} January 2020	18^{th} January 2020
15^{th} January 2020	18^{th} January 2020
21^{st} November 2022	1^{st} December 2022

2 Supplementary Figures

Open Research Section

Spectral analysis calculations were computed following Randel and Held (1991) using code from Jiménez-Esteve et al. (2022) which is available at `https://github.com/bernatj/paper_GRL_phase_locked_circumglobal_heat_extremes`.

Atmospheric blocks were detected following Schwierz et al. (2004) using the Steinfeld (2020) algorithm, which is available at `https://github.com/steidani/ConTrack`.

Copernicus Climate Change Service (C3S) (2017): ERA5: Fifth generation of ECMWF atmospheric reanalyses of the global climate. Copernicus Climate Change Service Cli-

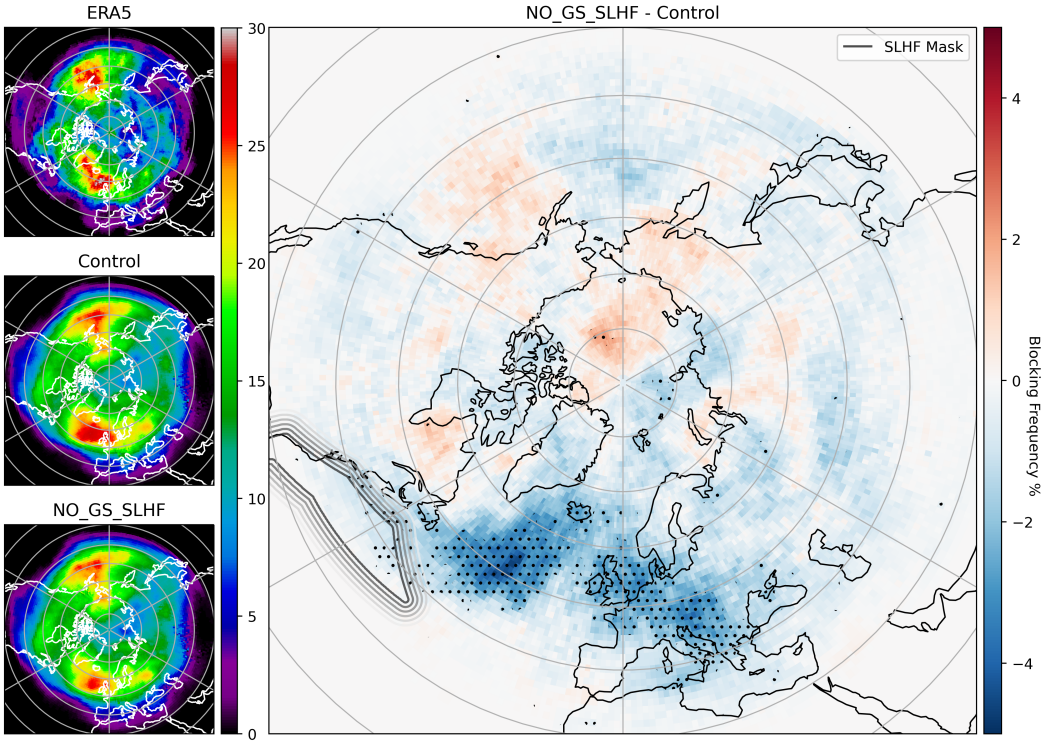

Figure 1. Mean blocking frequency for ERA5 (top left), the control run (middle left), the NO_GS_SLHF run (bottom left), and the difference between the NO_GS_SLHF and control runs (right) for the first two weeks of the reforecast. The grey contours indicate the SLHF mask applied, with the darkest (lightest) contour indicating complete suppression (permission). Stippling indicates areas that exceed the 95% confidence interval.

mate Data Store (CDS), date of access. `https://cds.climate.copernicus.eu/cdsapp\#!/home`

Acknowledgments

This project is part of EDIPI, which has received funding from the European Union's Horizon 2020 research and innovation programme under Marie Sklodowska-Curie grant No. 956396.

References

Jiménez-Esteve, B., Kornhuber, K., & Domeisen, D. (2022). Heat extremes driven by amplification of phase-locked circumglobal waves forced by topography in an idealized atmospheric model. *Geophysical Research Letters*, *49*(21), e2021GL096337.

Randel, W. J., & Held, I. m. (1991). Phase speed spectra of transient eddy fluxes and critical layer absorption. *Journal of the atmospheric sciences*, *48*(5), 688–697.

Schwierz, C., Croci-Maspoli, M., & Davies, H. (2004). Perspicacious indicators of atmospheric blocking. *Geophysical research letters*, *31*(6).

Steinfeld, D. (2020). *Contrack - contour tracking.* `https://github.com/steidani/ConTrack`. GitHub.

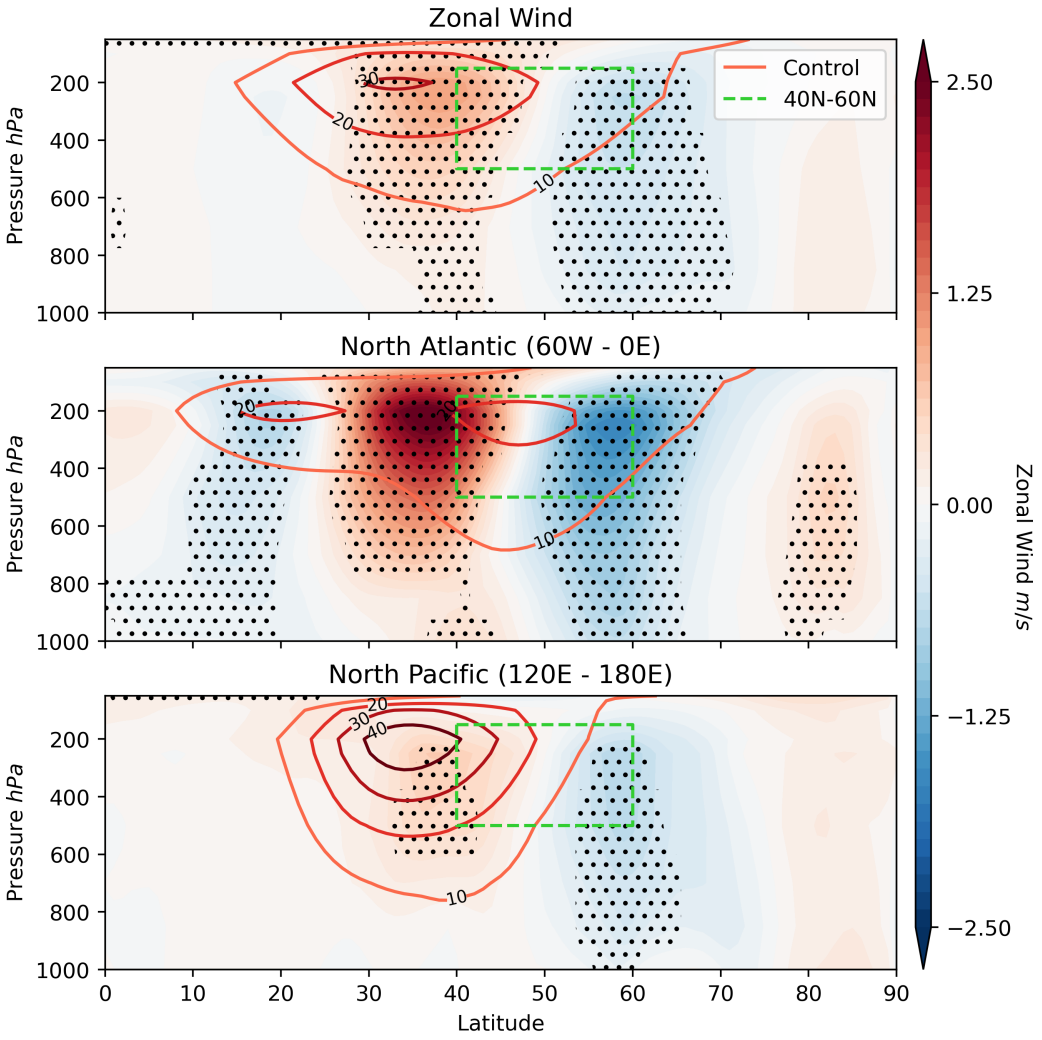

Figure 2. Meridional cross-section of the mean zonal wind for the entire Northern Hemisphere (top), the North Atlantic 60°W - 0°E (middle), and the North Pacific 120°E - 180°E (bottom). The control run is shown with the red contours, while the shading depicts the difference between the NO_GS_SLHF and the control runs. The dashed green box depicts the region where the spectral analysis is computed as in Supplementary Fig. 3.

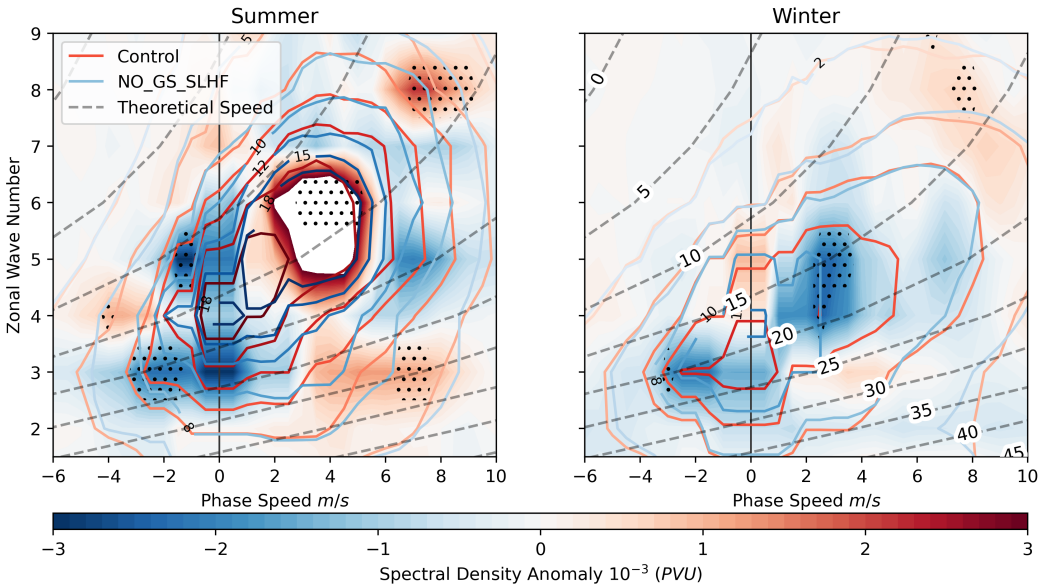

Figure 3. The power spectrum of the vertically averaged anomalous PV field from 500hPa to 150hPa within the latitudinal range of 40°N to 60°N for extended summer (left) and extended winter (right). The shading illustrates the difference between the NO_GS_SLHF and control runs, with the blue and red contours representing their respective reforecast means. The theoretical phase speed for different background flows at 40°N, applying a meridional wavenumber of 4, is depicted with grey dashed lines. Areas that exceed the 95% confidence interval are highlighted with stippling.

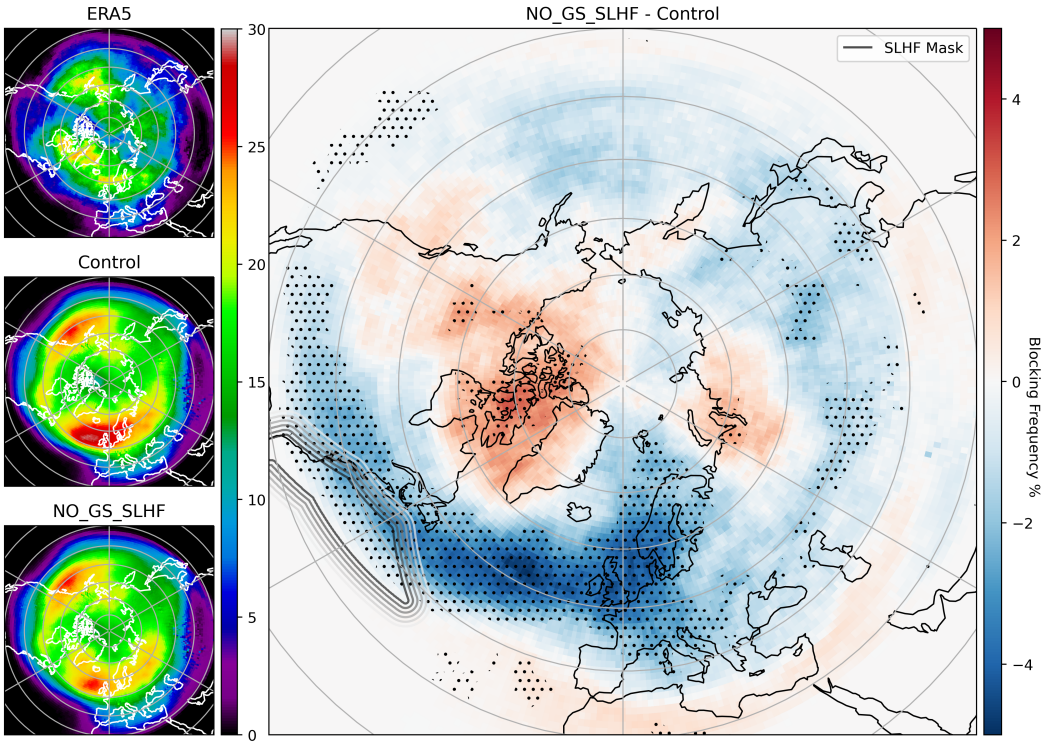

Figure 4. Mean blocking frequency for ERA5 (top left), the control run (middle left), the NO_GS_SLHF run (bottom left), and the difference between the NO_GS_SLHF and control runs (right) at resolution **Tco319**. The grey contours indicate the SLHF mask applied, with the darkest (lightest) contour indicating complete suppression (permission). Stippling indicates areas that exceed the 95% confidence interval.

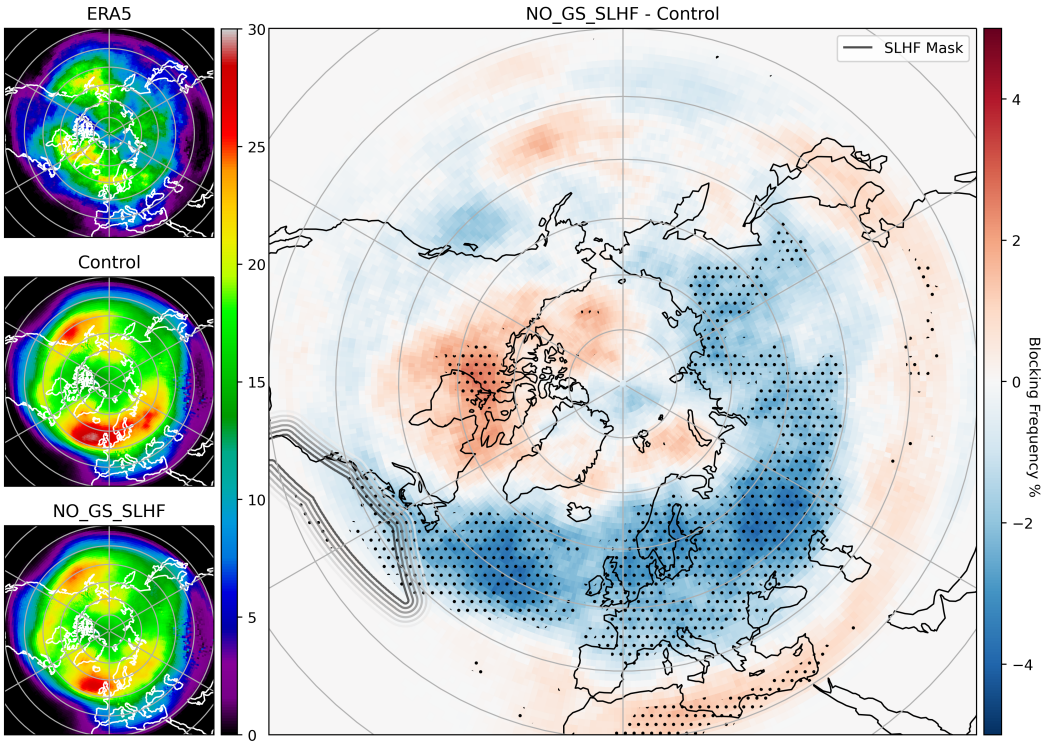

Figure 5. Mean blocking frequency for ERA5 (top left), the control run (middle left), the NO_GS_SLHF run (bottom left), and the difference between the NO_GS_SLHF and control runs (right) at resolution **Tco199**. The grey contours indicate the SLHF mask applied, with the darkest (lightest) contour indicating complete suppression (permission). Stippling indicates areas that exceed the 95% confidence interval.